

## P53 and HIS-tag Binding

Lindsey Barron and Alexander J. R. Bishop\*

Department of Cell Systems and Anatomy, Greehey Children's Cancer Research Institute, University of Texas Health at San Antonio, Texas, United States of America

### Abstract

P53 is a globular protein with distinct domains and a key tumor suppressor that functions through transcriptional transactivation, repression and protein-protein interactions. Numerous studies have implicated protein-protein interactions between p53 and a multitude of cellular proteins with a variety of known functions. Because of these interactions, and the many gene expression regulations, a multitude of potential mechanisms and their relationship to tumor suppression have been proposed. It is desirable to test these interactions in an *in vitro* setting to demonstrate that any identified interaction is direct. Due to the difficulties associated with purifying recombinant full-length p53, many studies have utilized the p53 DNA binding domain to test for direct protein interactions with p53. The DNA binding domain of p53 is structured, folds independently and dictates the stability of the full-length protein. Therefore, it is reasonable to perform *in vitro* experiments with this isolated domain. However, we demonstrate that if a HIS-tag is present on the interacting partner when testing for an interaction with p53, this can lead to detection of an artefactual protein-protein interaction raising the possibility of false positive results. Furthermore, the presence of the HIS-tag promotes aggregation and precipitation of the p53 DNA binding domain.

**Keywords:** p53; Protein purification; HIS-tag; Zinc

### Introduction

P53 is a sequence specific transcription factor that plays a critical role in regulating many cellular processes in response to a variety of stress signals [1]. These cellular processes include cell cycle arrest [2], senescence [3], apoptosis [4-7], DNA repair [8-11], and metabolism [12,13]. Additionally, p53 is considered one of the most important tumor suppressors as loss or mutation of p53 is found in approximately 50% of all human cancers [14]. Further, at least 80% of TP53 mutations map to the DNA binding domain (DBD), which underscores the importance of the p53<sup>DBD</sup> in tumor suppression [15].

The domain organization of full-length p53 includes a N-terminal transactivation domain (residues 1-62) [16], followed by a proline rich region (residues 63-94) [17,18], a central DNA-binding core domain (residues 94-312) [19], a C-terminal tetramerization domain (residues 325-356) [20], and a negative regulatory domain at the far C-terminus (residues 356-393) [21] (Figure S1). The N-terminal and C-terminal domains of p53 are both largely unstructured in their native states [22]. However, the DNA-binding domain and the tetramerization domains both fold into defined structures [23]. The structure of the p53<sup>DBD</sup> consists of an immunoglobulin-like central  $\beta$ -sandwich of two anti-parallel  $\beta$ -sheets. The  $\beta$ -sandwich serves as a scaffold to coordinate the DNA-binding surface that is composed of two loops (L2 and L3) that are stabilized by a zinc ion and a loop-sheet-helix motif (L1, S2 and S2', H2) [19]. Zinc-bound p53<sup>DBD</sup> is known as holo p53<sup>DBD</sup>, whereas p53<sup>DBD</sup> without bound zinc is known as apo p53<sup>DBD</sup> [24]. The single bound zinc ion present in holo p53<sup>DBD</sup> stabilizes the L2 and L3 loops and holds the L3 loop in the proper orientation for minor groove binding to DNA [19]. It has been suggested that a significant fraction of intracellular p53<sup>DBD</sup> may exist in the apo form due to the kinetics of zinc loss from p53<sup>DBD</sup> [24]. Apo p53<sup>DBD</sup> is less thermodynamically stable than holo p53<sup>DBD</sup> and more prone to precipitation [24]. Furthermore, it has been shown that apo p53<sup>DBD</sup> can inactivate holo p53<sup>DBD</sup> by converting soluble holo p53<sup>DBD</sup> into the aggregated form [24]. In fact, low intracellular zinc status is known to reduce the functionality of p53 as a gene transactivator [25].

Purification of the full-length p53 protein has proved challenging, due to its aggregation propensity and high content of disordered regions [23]. Because of the difficulties associated with purification of the full-length p53 protein and the importance of the p53<sup>DBD</sup> in tumor suppression, there have been a large number of reports using the p53<sup>DBD</sup> alone for *in vitro* experiments. This is a valid stratagem because the p53<sup>DBD</sup> adopts a well-defined conformation that folds independently of the N and C terminus [26]. Moreover, the p53<sup>DBD</sup> hot-spot mutations (most frequently mutated residues in p53 found in the human population (Figure S1) affect the stability of the full-length protein to the same extent that they affect the stability of the isolated DBD [27]. Thus, the DBD dictates the stability of the full-length protein and therefore the effect of mutation on p53<sup>DBD</sup> stability is a direct indication of the mutation-induced effect on the full-length protein [27].

Initially the p53<sup>DBD</sup> was extensively studied for its functions of DNA binding and transcriptional activation [16,28-31]. However, the role of the p53<sup>DBD</sup> in protein-protein interactions is steadily emerging as an equally important function of the domain [32]. Many studies have implicated protein-protein interactions between the p53<sup>DBD</sup> and various proteins that play critical regulatory roles. It is often desirable to assess whether or not these interactions are direct in an *in vitro* setting with purified recombinant proteins. Throughout our experiences working with the p53<sup>DBD</sup> in an *in vitro* setting, we discovered critical factors that affect the reliability of these results. Since these critical factors are components of commonly used procedures for producing recombinant proteins, we believe there is a need to caution researchers against using these procedures for producing recombinant p53<sup>DBD</sup>. Herein, we report

**\*Corresponding authors:** Alexander J. R. Bishop, Department of Cell Systems and Anatomy, Greehey Children's Cancer Research Institute, University of Texas Health at San Antonio, Texas, United States of America, Tel: 12105629060; E-mail: [bishopa@uthscsa.edu](mailto:bishopa@uthscsa.edu)

**Received** March 02, 2018; **Accepted** March 15, 2018; **Published** March 22, 2018

**Citation:** Barron L, Bishop AJR (2018) P53 and HIS-tag Binding. J Proteomics Bioinform 11: 062-067. doi: [10.4172/jpb.1000467](https://doi.org/10.4172/jpb.1000467)

**Copyright:** © 2018 Barron L, et al. This is an open-access article distributed under the terms of the Creative Commons Attribution License, which permits unrestricted use, distribution, and reproduction in any medium, provided the original author and source are credited.

a method to consistently produce soluble folded p53<sup>DBD</sup>. Additionally, we describe the deleterious effects of the commonly used 6x histidine tag (HIS-tag) when performing *in-vitro* experiments with the p53<sup>DBD</sup>.

## Material and Methods

### *E. coli* expression constructs and cell line

The wild-type DNA binding domain (DBD) of human p53 (amino acids 94-312) was subcloned into the pET-15b vector (Stratagene) following restriction enzyme digestion with *NdeI* and *BglIII*. The construct allowed for expression of a 6x HIS-tag fusion protein with the HIS-tag at the N-terminus. Additionally, the construct contained a thrombin cleavage site (LVPRGS) after the 6 histidine residues and before the first codon of the human p53<sup>DBD</sup>.

### Minimal media preparation

1 L of minimal media contained 100 mL of 10X M9 salts (60 g/L Na<sub>2</sub>HPO<sub>4</sub>, 30 g/L KH<sub>2</sub>PO<sub>4</sub>, 5 g/L NaCl, pH 7.4), 12.5 mL of 20% (weight/volume) D-glucose, 10 mL of 100 g/L N<sup>15</sup>H<sub>4</sub>Cl, 1 mg biotin, 0.5 mL 2 mg/mL thiamine hydrochloride, 2 mL 1M MgSO<sub>4</sub>, 0.2 mL 0.5M CaCl<sub>2</sub>, 1 mL 15 mg/mL FeCl<sub>2</sub> in 1M HCl, 1 mL 15 mg/mL ZnCl<sub>2</sub> in water, 2 mL 10% (weight/volume) yeast extract and carbenicillin added to a final concentration of 100 µg/mL. The carbenicillin, N<sup>15</sup>H<sub>4</sub>Cl, thiamine hydrochloride, FeCl<sub>2</sub> and ZnCl<sub>2</sub> were filtered through a 0.2 µm filter for sterilization. The remaining components were autoclaved for sterilization. All components were added to 900 mL of water and the solution was mixed thoroughly after each addition. Following addition of all components the pH of the media was adjusted to pH=7.4.

### Protein expression and growth conditions

The human p53<sup>DBD</sup> DNA was transformed into *E. coli* BL-21 (DE3) gold cells using a standard heat shock procedure and plated on LB agar containing 100 µg/mL of carbenicillin. Colonies were suspended in minimal media, used to inoculate 1 L of minimal media and grown at 37°C until an OD<sub>600</sub> of 0.2 was reached. The temperature was then lowered to 20°C and expression induced with 0.8 mM IPTG when the OD<sub>600</sub> reached 0.6. Eighteen hours after IPTG induction the culture was centrifuged at 3629 x g for 10 minutes. The supernatant was decanted and the cell pellet was stored at -20°C until purification.

### Purification of recombinant human p53 DNA binding domain

A cell pellet from a 1 L culture was resuspended in 120 mL lysis buffer (25 mM NaH<sub>2</sub>PO<sub>4</sub> pH 7.2, 300 mM NaCl, 5 mM imidazole) supplemented with EDTA-free protease inhibitor (Roche). The lysate was then sonicated on ice at 20% amplitude for a 2 min cycle with a pulse of 1 second on and 1 second off, followed by four 1 minute cycles with a pulse of 1 second on and 1 second off. The lysate was then cleared by centrifugation at 31,360 x g for 20 minutes at 4°C. All subsequent steps were performed at 4°C with buffers that were equilibrated to 4°C. The cleared lysate was then applied to a 30 mL Ni-NTA (Pierce) column by gravity flow. Prior to application of the lysate, the Ni-NTA column was washed with 100 mL water and equilibrated with 200 mL lysis buffer that did not contain protease inhibitor. After application of the lysate, the column was first washed with 100 mL lysis buffer (without protease inhibitor) which was followed with an additional 100 mL wash of lysis buffer containing 20 mM imidazole. The protein was then eluted in 10 mL fractions with 25 mM NaH<sub>2</sub>PO<sub>4</sub> pH 7.2, 50 mM NaCl, 300 mM imidazole. Protein containing fractions were assessed by SDS-PAGE and Coomassie staining. The fractions determined to contain

protein were pooled, treated with thrombin (4 units of thrombin per milligram of protein) and put into dialysis (10 kDa molecular weight cut off dialysis membrane) against 25 mM Tris pH 7.2, 5 mM DTT and 10% glycerol. The thrombin cleavage and dialysis was conducted for 18 hours at 4°C. The HIS-tag cleaved protein was then applied to a 5 mL SP-HP sepharose cation exchange column (GE). A linear salt gradient (with 25 mM Tris pH 7.2 as buffer A and 25 mM Tris pH 7.2, 1 M NaCl as buffer B) at a flow-rate of 2 mL/min over 24 column volumes was used to elute the protein and 2 mL fractions were collected. Protein containing fractions were assessed and purity confirmed by SDS-PAGE and Coomassie staining.

### Protein quantification

The concentration of purified p53<sup>DBD</sup> was determined by dividing the absorbance at 280 nm by the extinction coefficient for p53<sup>DBD</sup> (15930 M<sup>-1</sup> cm<sup>-1</sup>). The extinction coefficient was estimated by the method of Gill and von Hippel [33].

### 2D 1H-15N heteronuclear single quantum coherence (HSQC)

N<sup>15</sup> ammonium chloride was used to selectively label p53<sup>DBD</sup> for these experiments. Pure p53<sup>DBD</sup> was buffer exchanged into 25 mM NaH<sub>2</sub>PO<sub>4</sub> pH 7.2, 150 mM NaCl, 5 mM DTT and 5% D<sub>2</sub>O and concentrated to 80 µM. 2D <sup>1</sup>H-<sup>15</sup>N heteronuclear single quantum coherence (HSQC) spectra were collected on a Bruker Avance 600 spectrometer equipped with a 5 mM TXI cryoprobe. Spectra were collected at 293 K with 32 scans. The data was processed with NMRPipe [34] and analyzed with Sparky (Goddard and Kneller, SPARKY 3, University of California, San Francisco).

### Precipitation test

A cell pellet from a 500 mL culture grown in zinc-supplemented minimal medium was purified via Ni-NTA chromatography as described above in the purification of recombinant human p53 DNA binding domain section. Following elution from the Ni-NTA column, the eluate was mixed to homogeneity and divided into 4 samples containing 1 mL of HIS-p53<sup>DBD</sup>. 4 units of thrombin was added to the +thrombin samples. The samples were dialyzed overnight at 4°C in buffer containing 25 mM Tris pH 7.2, 10% glycerol with and without DTT. The next morning the precipitate was pelleted by centrifugation at 10,000 x g for 5 min. The concentration of soluble p53<sup>DBD</sup> that remained in the supernatant was quantified by dividing the absorbance at 280 nm by the extinction coefficient for p53<sup>DBD</sup> (15930 M<sup>-1</sup> cm<sup>-1</sup>). The experiment was performed in triplicate and statistically significant differences between the + and - thrombin samples were determined by 1-way ANOVA.

### *In-vitro* coimmunoprecipitation

1 µM recombinant untagged p53<sup>DBD</sup> (expressed in zinc-supplemented growth medium) was incubated with either 1 µM recombinant HIS-tagged GFP (BPS biosciences) (C-terminal 6x HIS-tag), 1 µM non-tagged GFP (Abcam) or alone in 25 mM NaH<sub>2</sub>PO<sub>4</sub> pH 7.2, 150 mM NaCl, 1% Triton-X 100. 30 µL of protein A/G agarose beads (Pierce) that were prebound with 2 µg of either rabbit anti-GFP (Abcam) or nonspecific rabbit IgG (Cell Signaling) and preblocked with 10% bovine serum albumin (BSA) were then added to each sample in a total volume of 500 µL. The samples were then incubated overnight (18 hours) at 4°C. The beads were then pelleted by centrifugation and the supernatant was removed. The beads were washed four times with 25 mM NaH<sub>2</sub>PO<sub>4</sub> pH 7.2, 150 mM NaCl, 1% Triton-X 100. Protein was then eluted by resuspending the beads in 30 µL Laemmli buffer

and boiling at 95°C for 5 minutes. The beads were then pelleted. 15  $\mu$ L of the supernatant was resolved by SDS-PAGE and transferred to a nitrocellulose membrane. The membrane was subsequently probed with a polyclonal sheep anti-p53 (Calbiochem) at a dilution of 1:2500 and a monoclonal mouse anti-GFP (Santa Cruz) at a dilution of 1:1000. The experiment was performed in triplicate and the ratio of p53<sup>DBD</sup>:HIS-GFP and p53<sup>DBD</sup>:GFP in the immunoprecipitate was quantified with ImageJ software [35]. 1-way ANOVA was performed to determine a statistically significant difference between the ratio of p53<sup>DBD</sup>:HIS-GFP versus p53<sup>DBD</sup>:GFP.

## Results

### Presence of the HIS-tag promotes p53DBD aggregation

In order to study p53<sup>DBD</sup> protein interactions we worked to establish the production of recombinant protein. Unfortunately, attempts to produce stable, soluble HIS-p53<sup>DBD</sup> from recombinant proteins expressed in *E. coli* proved to be challenging. While we were able to recover reasonable yields of pure protein with immobilized-metal affinity chromatography followed by cation exchange chromatography, we had a persistent problem with protein solubility. Initially, we attempted to prevent the precipitation with the commonly employed strategies of addition of glycerol and/or arginine and dilution of the protein [36]. However, using these strategies to keep the protein in solution severely limited the potential for downstream applications. Furthermore, when we attempted to collect a 2D <sup>1</sup>H-<sup>15</sup>N Heteronuclear single quantum coherence (HSQC) spectrum of p53<sup>DBD</sup> (expressed in zinc-supplemented growth medium) in buffer containing 75 mM arginine (which we found worked well to solubilize the protein) we obtained a spectrum where all of the backbone amide signals were clustered between 7.8 – 8.5 ppm (Figure 1A), rather than dispersed beyond the random coil region in a unique manner as previously reported for holo p53<sup>DBD</sup> [37]. Thus, the purified p53<sup>DBD</sup> was unfolded or aggregated and we set out to investigate potential sources that may cause this.

Since the p53<sup>DBD</sup> contains a zinc finger [19] and the imidazole ring of histidine residues has affinity for divalent cations such as zinc [38], we decided to investigate the possibility that the HIS-tag on the p53<sup>DBD</sup> fusion protein was causing the observed protein aggregation. We therefore prepared two samples of p53<sup>DBD</sup> (expressed in zinc-supplemented growth medium) at equal molar concentrations. One sample was treated with thrombin protease to remove the HIS-tag and the other sample was left untreated. Both samples were then incubated overnight at 4°C. The next morning the samples were inspected for precipitate as an indication of protein aggregation. A large amount of precipitate was observed in the sample where the HIS-tag was intact. However, the amount of precipitate was significantly reduced in the sample where the tag was removed (Figure 1B). This result strongly suggested that the presence of the HIS-tag on p53<sup>DBD</sup> promoted precipitation/aggregation of the protein.

After observing such a substantial difference in the amount of precipitate present in the presence versus absence of the HIS-tag, we again attempted to collect a 2D <sup>1</sup>H-<sup>15</sup>N HSQC spectrum of untagged p53<sup>DBD</sup> (expressed in zinc-supplemented growth medium). Since removal of the HIS-tag resolved the precipitation problem, we were able to collect this spectrum in buffer that did not contain arginine. A marked improvement in spectra was observed upon removal of the HIS-tag, as a spectrum with a unique dispersed pattern of chemical shifts characteristic of a folded protein that is not aggregating was obtained (Figure 1C). Furthermore, the spectrum obtained is consistent with that previously reported for the p53<sup>DBD</sup> [35].

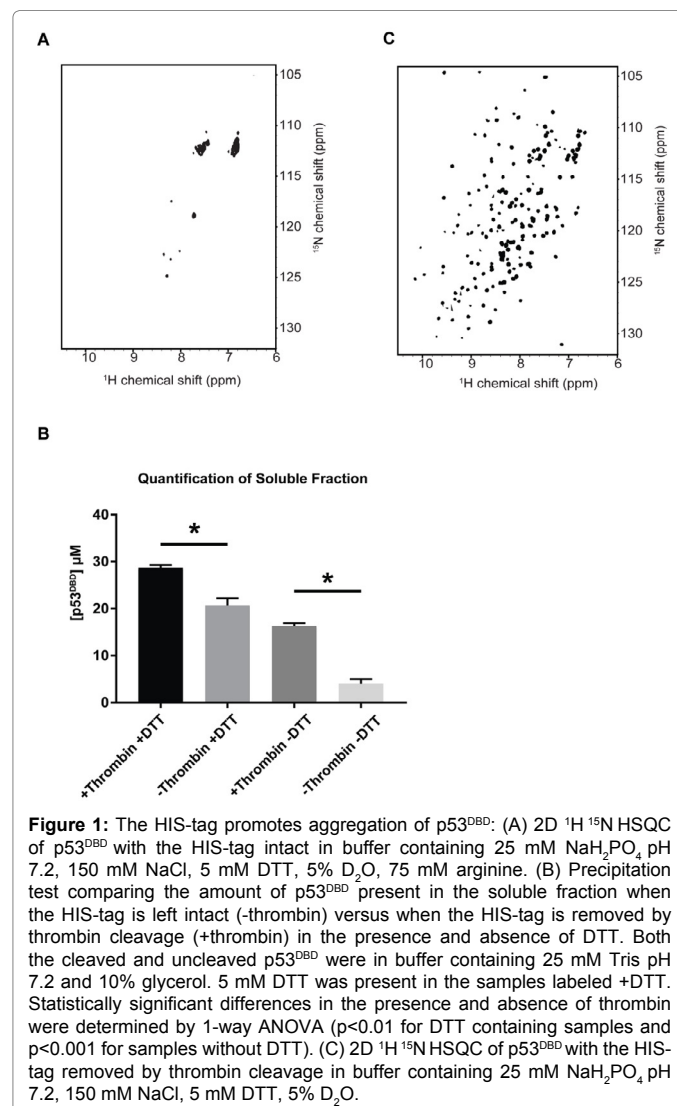


**Figure 1:** The HIS-tag promotes aggregation of p53<sup>DBD</sup>. (A) 2D <sup>1</sup>H <sup>15</sup>N HSQC of p53<sup>DBD</sup> with the HIS-tag intact in buffer containing 25 mM NaH<sub>2</sub>PO<sub>4</sub> pH 7.2, 150 mM NaCl, 5 mM DTT, 5% D<sub>2</sub>O, 75 mM arginine. (B) Precipitation test comparing the amount of p53<sup>DBD</sup> present in the soluble fraction when the HIS-tag is left intact (-thrombin) versus when the HIS-tag is removed by thrombin cleavage (+thrombin) in the presence and absence of DTT. Both the cleaved and uncleaved p53<sup>DBD</sup> were in buffer containing 25 mM Tris pH 7.2 and 10% glycerol. 5 mM DTT was present in the samples labeled +DTT. Statistically significant differences in the presence and absence of thrombin were determined by 1-way ANOVA ( $p < 0.01$  for DTT containing samples and  $p < 0.001$  for samples without DTT). (C) 2D <sup>1</sup>H <sup>15</sup>N HSQC of p53<sup>DBD</sup> with the HIS-tag removed by thrombin cleavage in buffer containing 25 mM NaH<sub>2</sub>PO<sub>4</sub> pH 7.2, 150 mM NaCl, 5 mM DTT, 5% D<sub>2</sub>O.

### Zinc supplementation of *E. coli* growth medium is essential to the production of p53DBD

After observing that the presence of the HIS-tag on p53<sup>DBD</sup> was promoting precipitation of the protein we attempted to purify p53<sup>DBD</sup> that was expressed in *E. coli* grown in Lysogeny Broth (LB) medium at room temperature. However, before we could remove the HIS-tag by thrombin cleavage the protein started to precipitate. We did not observe this rapid precipitation when the protein was expressed in *E. coli* grown in minimal media and purified at room temperature. When minimal media was used we were able to successfully remove the HIS-tag before the protein precipitated and thus were able to successfully keep the protein in solution thereafter.

Since we noticed a substantial difference in precipitation kinetics when LB was used as the growth medium we looked into potential reasons for this difference. We noted that zinc is not added to the LB medium, while our minimal medium recipe includes ZnCl<sub>2</sub> at a final concentration of 15  $\mu$ g/mL. Therefore, we reasoned that the observed precipitation was likely a result of insufficient zinc. We suspected that the lack of zinc supplementation was leading to expression of p53<sup>DBD</sup> primarily in the zinc-free form (apo p53<sup>DBD</sup>), since apo p53<sup>DBD</sup> is

thermodynamically less stable and more prone to precipitation than holo p53<sup>DBD</sup> [24].

We decided to test the effect of zinc supplementation of the growth medium by purifying p53<sup>DBD</sup> expressed in *E. coli* grown in minimal media supplemented with 15 µg/mL zinc and comparing that to purified p53<sup>DBD</sup> expressed in *E. coli* grown in minimal media where zinc was not added. These proteins were purified at 4°C which we found improved the stability of the p53<sup>DBD</sup>. Thus, this improvement in stability allowed for removal of the HIS-tag from the p53<sup>DBD</sup> protein purified from minimal media that did not receive zinc supplementation. Both proteins were purified from 500 mL of *E. coli* culture using identical procedures. However a difference in yield, cation-exchange chromatograms and appearance on SDS-PAGE was observed (Figure 2A-F). The fractions constituting the peak at a conductivity of 26.5 mS/cm were pooled and used for the subsequent NMR experiments. We then collected 2D <sup>1</sup>H-<sup>15</sup>N HSQC spectra with p53<sup>DBD</sup> that received zinc supplementation and p53<sup>DBD</sup> that did not receive zinc supplementation. We prepared both NMR samples at the same concentration (80 µM) and collected the same number of scans for the 2D <sup>1</sup>H-<sup>15</sup>N HSQC spectra of each protein. We noticed a difference in spectra for the protein that received zinc supplementation compared to the protein that did not (Figure 3A), which was not due to protein concentration (Figure 3B). While a high degree of spectral overlap was observed for the two proteins, there was a significant loss in signal intensity for approximately 35 residues (Figure 3C). This suggests that while the majority of the structure is maintained in the protein that did not receive zinc supplementation there is local structural perturbation. While these experiments can not conclude that apo p53<sup>DBD</sup> is present, the result is consistent with a high degree of structural fluctuation in the L2 and L3 loops expected in the absence of zinc (Figure 3D).

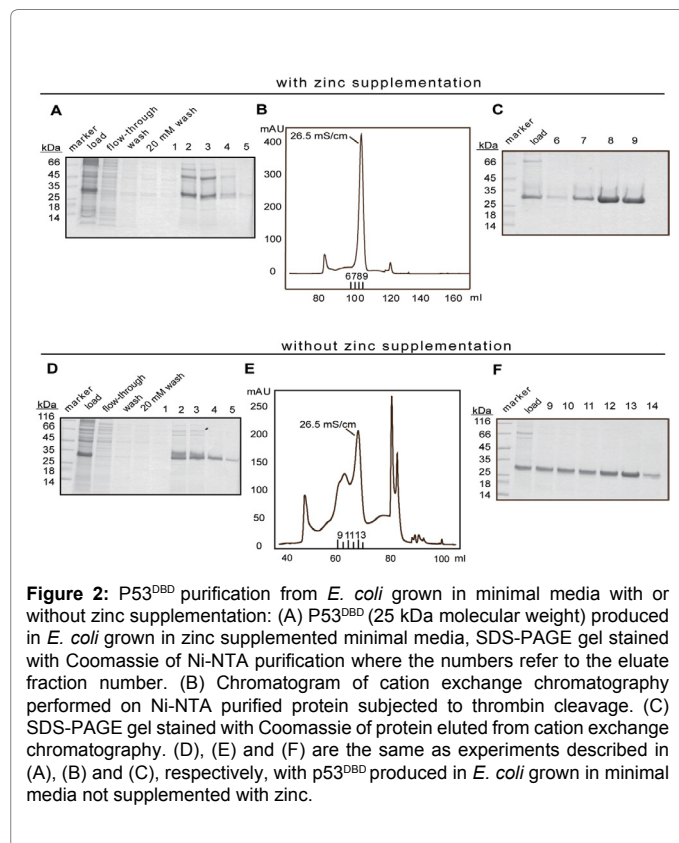


**Figure 2:** P53<sup>DBD</sup> purification from *E. coli* grown in minimal media with or without zinc supplementation: (A) P53<sup>DBD</sup> (25 kDa molecular weight) produced in *E. coli* grown in zinc supplemented minimal media, SDS-PAGE gel stained with Coomassie of Ni-NTA purification where the numbers refer to the eluate fraction number. (B) Chromatogram of cation exchange chromatography performed on Ni-NTA purified protein subjected to thrombin cleavage. (C) SDS-PAGE gel stained with Coomassie of protein eluted from cation exchange chromatography. (D), (E) and (F) are the same as experiments described in (A), (B) and (C), respectively, with p53<sup>DBD</sup> produced in *E. coli* grown in minimal media not supplemented with zinc.

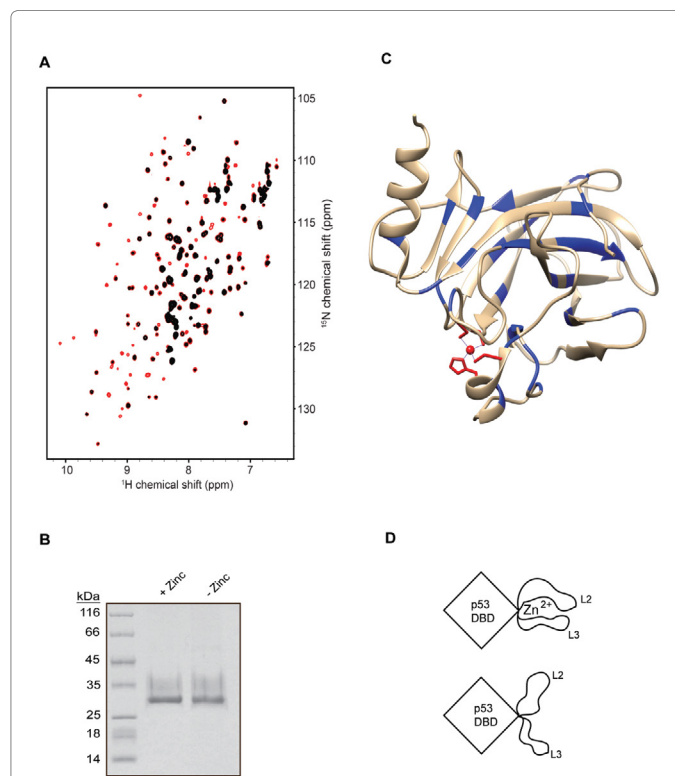


**Figure 3:** 2D <sup>1</sup>H<sup>15</sup>N HSQC of p53<sup>DBD</sup> from *E. coli* grown with and without zinc supplementation: (A) Overlay of 2D <sup>1</sup>H<sup>15</sup>N HSQC spectra of p53<sup>DBD</sup> that received zinc supplementation (red) and p53<sup>DBD</sup> that did not receive zinc supplementation (black). (B) SDS-PAGE gel stained with Coomassie of a 1:10 dilution of the samples used to obtain the 2D <sup>1</sup>H<sup>15</sup>N HSQC spectra. (C) Ribbon diagram of the structure of p53<sup>DBD</sup>. Residues with a loss of signal intensity in the absence of zinc are colored blue. The zinc ion is depicted as a red sphere. The diagram was generated with Chimera software [39] (PDB ID code 2AH1). (D) Schematic diagram illustrating the expected structural perturbations of p53<sup>DBD</sup> in the absence of the zinc ion.

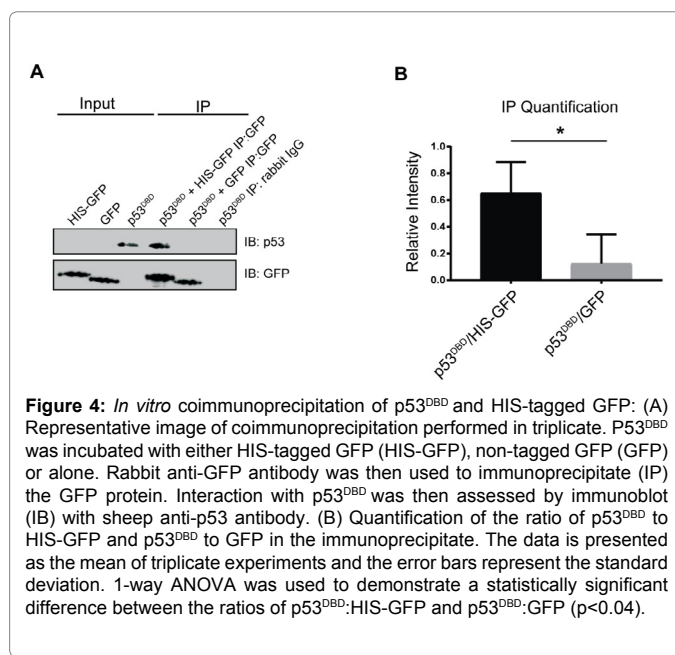


**Figure 4:** *In vitro* coimmunoprecipitation of p53<sup>DBD</sup> and HIS-tagged GFP: (A) Representative image of coimmunoprecipitation performed in triplicate. P53<sup>DBD</sup> was incubated with either HIS-tagged GFP (HIS-GFP), non-tagged GFP (GFP) or alone. Rabbit anti-GFP antibody was then used to immunoprecipitate (IP) the GFP protein. Interaction with p53<sup>DBD</sup> was then assessed by immunoblot (IB) with sheep anti-p53 antibody. (B) Quantification of the ratio of p53<sup>DBD</sup> to HIS-GFP and p53<sup>DBD</sup> to GFP in the immunoprecipitate. The data is presented as the mean of triplicate experiments and the error bars represent the standard deviation. 1-way ANOVA was used to demonstrate a statistically significant difference between the ratios of p53<sup>DBD</sup>:HIS-GFP and p53<sup>DBD</sup>:GFP (p<0.04).

## Utilization of HIS-tagged proteins can lead to the identification of artefactual protein-protein interactions with p53<sup>DBD</sup>

Two possible hypotheses exist to explain the p53<sup>DBD</sup> aggregation observed in the presence of the HIS-tag. The aggregation could be a result of intermolecular interactions between the p53<sup>DBD</sup> zinc finger and the HIS-tag or from HIS-tag chelation of zinc. Since the former hypothesis raises the possibility that artefactual interactions could be detected between p53 and a HIS-tagged interacting partner, we attempted to demonstrate an interaction between p53<sup>DBD</sup> and an irrelevant protein that should have no biological purpose for an interaction with p53<sup>DBD</sup>. We chose green fluorescent protein (GFP) and investigated if we could detect an interaction between p53<sup>DBD</sup> (expressed in zinc supplemented medium) and a HIS-tagged GFP by *in vitro* coimmunoprecipitation. We also performed coimmunoprecipitations with p53<sup>DBD</sup> and nontagged-GFP as well as nonspecific rabbit IgG to serve as negative controls. As we predicted, we detected an interaction between p53<sup>DBD</sup> and HIS-GFP that was enriched relative to the non-tagged-GFP and nonspecific IgG controls (Figure 4). Based on this result, we argue that HIS-tags on the interacting partner should be avoided when attempting to demonstrate an interaction with p53. Additionally, we conclude that a HIS-tag should be avoided in all experiments that involve p53 in general as it can have major effects on the consistency and validity of results.

## Discussion

Utilization of HIS-tags for affinity chromatography and LB as *E. coli* growth medium are two commonly employed strategies for purification of recombinant proteins [36,39,40]. These strategies are widely used without consideration of the potential impact on the resulting protein. The HIS-tag is often left on proteins after purification as it is a small tag and generally viewed as inconsequential [36]. However, we demonstrate that the presence of the HIS-tag can have detrimental consequences when used in experiments involving a zinc finger containing protein. Furthermore, we emphasize that the components of the growth medium need to be considered in order to produce properly structured proteins.

The typical composition of LB medium purchased from manufacturers is tryptone, yeast extract and NaCl [41]. These formulations contain only trace amounts of divalent cations including zinc. We demonstrate that a lack of zinc supplementation can affect the structure of recombinant p53<sup>DBD</sup> expressed in and purified from *E. coli* grown in medium such as LB, which contains only low concentrations of zinc. We observed a loss of NMR signal intensity when we compared p53<sup>DBD</sup> purified from *E. coli* grown in media that received zinc supplementation versus non-supplemented media. The loss of signal intensity observed is consistent with local structural perturbation that would be expected from a high degree of structural fluctuation of the L2 and L3 loops when zinc is not present [42]. The zinc ion present in the p53<sup>DBD</sup> is known to coordinate and stabilize these loops in order to form the DNA binding surface and in its absence the p53<sup>DBD</sup> binds DNA non-specifically [24]. Therefore, the presence of the zinc ion and thus the production of holo p53<sup>DBD</sup> is critical for site-specific DNA binding. Moreover, the increased structural fluctuation of p53<sup>DBD</sup> in the absence of zinc could affect the results of experiments testing for potential protein-protein interactions with p53. For the aforementioned reasons, we note that zinc supplementation of the media needs to be considered when drawing conclusions from *in vitro* experiments with purified recombinant p53<sup>DBD</sup>. If the media lacks zinc supplementation, then the experiment is likely testing apo p53<sup>DBD</sup> and the interpretations of the results need to be adjusted accordingly. In addition, it is important to note that excess concentrations of zinc should be avoided when handling this protein as excess zinc causes p53<sup>DBD</sup> precipitation [24].

We provide compelling evidence that the presence of the HIS-tag on p53<sup>DBD</sup> is problematic as it promotes the precipitation and aggregation of p53<sup>DBD</sup>. We believe it is important to remove the HIS-tag from p53<sup>DBD</sup> immediately after purification on a Ni-NTA column in order to avoid the negative consequences from the tag. Removal of the HIS-tag greatly improves the solubility of purified recombinant p53<sup>DBD</sup>. Beyond the problems that the HIS-tag causes for solubility, it also affects the reproducibility and accuracy of results. We showed that by simply adding a HIS-tag on GFP we can detect an interaction between p53<sup>DBD</sup> and GFP. The interaction between p53<sup>DBD</sup> and GFP was diminished in the absence of the HIS-tag. This result casts doubt on studies demonstrating a direct interaction between p53 and a HIS-tagged protein [43-46]. The interactions shown in these experiments could result from a true direct interaction or from artificial dimer formation between the HIS-tag and p53 zinc finger. As additional pieces of evidence in support of the interaction are presented in these studies, it is likely that the direct interactions are real. However, we believe it is important that this caveat is reported in the literature so that researchers avoid uncertainty associated with using HIS-tagged proteins to study direct interactions with p53. Moreover, the protein aggregation observed in the presence of the HIS-tag could lead to a loss of the protein and erroneous negative results. Therefore, we urge researchers to refrain from using HIS-tagged proteins when studying p53. The HIS-tag should be avoided on p53 and on any other protein that is being studied in relation to p53 as the deleterious effects would occur in either scenario. Additionally, these results likely extend to and should be considered when working with any zinc finger containing protein.

In conclusion, we believe that the HIS-tag and LB growth medium are widely used for recombinant protein purification without consideration of how their use affects the quality of the purified protein and the subsequent experimental results. The experiments demonstrating the negative impacts of the HIS-tag and growth medium lacking zinc supplementation on p53<sup>DBD</sup> purification are significant because they provide explicit evidence of how such seemingly minor details can greatly impact results. Quite often, researchers work quickly or work with what's in solution when working with "intrinsically" unstable proteins to overcome stability issues. We counter that perhaps some of these proteins can be stabilized by simple inclusion of sufficient concentrations of divalent cations or removal of the HIS-tag.

## Acknowledgements

We acknowledge the Biomolecular NMR Core at UT Health at San Antonio which is supported by Mays Cancer Center P30 Grant CA054174, CPRIT grant RP120867, and Texas State funds provided through the Office of the VPR of UT Health at San Antonio. We especially thank Dr. Kristin Cano for her invaluable assistance in setting up, analyzing and interpreting the NMR experiments. We thank Dr. Andrew P. Hinck for insights as to the potential causes of the insolubility and lack of NMR signals and for providing the laboratory resources that enabled the preparation and purification of the samples used for NMR. Funding was by the NIH (K22ES012264, 1R15ES019128 and 1R01CA152063), Voelcker Fund Young Investigator Award, CPRIT (RP150445) and ACS (RSG-10-049-01-DMC) to AJRB. L. Barron was supported by a CPRIT Research Training Award (RP170345) and an IRACDA Grant (K12GM111726).

## References

1. Speidel D (2015) The role of DNA damage responses in p53 biology. Arch Toxicol 89: 501-517.
2. Kastan MB, Zhan Q, el-Deiry WS, Carrier F, Jacks T, et al. (1992) A mammalian cell cycle checkpoint pathway utilizing p53 and GADD45 is defective in ataxia-telangiectasia. Cell 71: 587-597.
3. Chang BD, Xuan Y, Broude EV, Zhu H, Schott B, et al. (1999) Role of p53 and p21waf1/cip1 in senescence-like terminal proliferation arrest induced in human tumor cells by chemotherapeutic drugs. Oncogene 18: 4808-4818.

4. Miyashita T, Reed JC (1995) Tumor suppressor p53 is a direct transcriptional activator of the human bax gene. *Cell* 80: 293-299.
5. Yu J, Zhang L, Hwang PM, Kinzler KW, Vogelstein B (2001) PUMA induces the rapid apoptosis of colorectal cancer cells. *Mol Cell* 7: 673-682.
6. Mihara M, Erster S, Zaika A, Petrenko O, Chittenden T, et al. (2003) p53 has a direct apoptogenic role at the mitochondria. *Mol Cell* 11: 577-590.
7. Oda E, Ohki R, Murasawa H, Nemoto J, Shibue T, et al. (2000) Noxa, a BH3-only member of the Bcl-2 family and candidate mediator of p53-induced apoptosis. *Science* 288: 1053-1058.
8. Ford JM, Hanawalt PC (1997) Expression of wild-type p53 is required for efficient global genomic nucleotide excision repair in UV-irradiated human fibroblasts. *J Biol Chem* 272: 28073-28080.
9. Chen J, Sadowski I (2005) Identification of the mismatch repair genes PMS2 and MLH1 as p53 target genes by using serial analysis of binding elements. *Proc Natl Acad Sci U S A* 102: 4813-4818.
10. Gatz SA, Wiesmuller L (2006) p53 in recombination and repair. *Cell Death Differ* 13: 1003-1016.
11. de Souza-Pinto NC, Harris CC, Bohr VA (2004) p53 functions in the incorporation step in DNA base excision repair in mouse liver mitochondria. *Oncogene* 23: 6559-6568.
12. Schwartzberg-Bar-Yoseph F, Armoni M, Karnieli E (2004) The tumor suppressor p53 down-regulates glucose transporters GLUT1 and GLUT4 gene expression. *Cancer Res* 64: 2627-2633.
13. Maddocks OD, Vousden KH (2011) Metabolic regulation by p53. *J Mol Med (Berl)* 89: 237-245.
14. Cheok CF, Verma CS, Baselga J, Lane DP (2011) Translating p53 into the clinic. *Nat Rev Clin Oncol* 8: 25-37.
15. Olivier M, Hollstein M, Hainaut P (2010) TP53 mutations in human cancers: origins, consequences, and clinical use. *Cold Spring Harb Perspect Biol* 2: a001008.
16. Fields S, Jang SK (1990) Presence of a potent transcription activating sequence in the p53 protein. *Science* 249: 1046-1049.
17. Walker KK, Levine AJ (1996) Identification of a novel p53 functional domain that is necessary for efficient growth suppression. *Proc Natl Acad Sci U S A* 93: 15335-15340.
18. Muller-Tiemann BF, Halazonetis TD, Elting JJ (1998) Identification of an additional negative regulatory region for p53 sequence-specific DNA binding. *Proc Natl Acad Sci U S A* 95: 6079-6084.
19. Cho Y, Gorina S, Jeffrey PD, Pavletich NP (1994) Crystal structure of a p53 tumor suppressor-DNA complex: understanding tumorigenic mutations. *Science* 265: 346-355.
20. Jeffrey PD, Gorina S, Pavletich NP (1995) Crystal structure of the tetramerization domain of the p53 tumor suppressor at 1.7 angstroms. *Science* 267: 1498-1502.
21. Ahn J, Prives C (2001) The C-terminus of p53: the more you learn the less you know. *Nat Struct Biol* 8: 730-732.
22. Bell S, Klein C, Muller L, Hansen S, Buchner J, et al. (2002) p53 contains large unstructured regions in its native state. *J Mol Biol* 322: 917-927.
23. Joerger AC, Fersht AR (2007) Structure-function-rescue: the diverse nature of common p53 cancer mutants. *Oncogene* 26: 2226-2242.
24. Butler JS, Loh SN (2003) Structure, function, and aggregation of the zinc-free form of the p53 DNA binding domain. *Biochemistry* 42: 2396-2403.
25. Ho E, Ames BN (2002) Low intracellular zinc induces oxidative DNA damage, disrupts p53, NFkappa B, and AP1 DNA binding, and affects DNA repair in a rat glioma cell line. *Proc Natl Acad Sci U S A* 99: 16770-16775.
26. Pavletich NP, Chambers KA, Pabo CO (1993) The DNA-binding domain of p53 contains the four conserved regions and the major mutation hot spots. *Genes Dev* 7: 2556-2564.
27. Bullock AN, Henckel J, DeDecker BS, Johnson CM, Nikolova PV, et al. (1997) Thermodynamic stability of wild-type and mutant p53 core domain. *Proc Natl Acad Sci U S A* 94: 14338-14342.
28. Unger T, Nau MM, Segal S, Minna JD (1992) p53: a transdominant regulator of transcription whose function is ablated by mutations occurring in human cancer. *EMBO J* 11: 1383-1390.
29. Kern SE, Pietsenpol JA, Thiagalingam S, Seymour A, Kinzler KW, et al. (1992) Oncogenic forms of p53 inhibit p53-regulated gene expression. *Science* 256: 827-830.
30. Farmer G, Bargonetti J, Zhu H, Friedman P, Prywes R, et al. (1992) Wild-type p53 activates transcription in vitro. *Nature* 358: 83-86.
31. Friedlander P, Haupt Y, Prives C, Oren M (1996) A mutant p53 that discriminates between p53-responsive genes cannot induce apoptosis. *Mol Cell Biol* 16: 4961-4971.
32. Fernandez-Fernandez MR, Sot B (2011) The relevance of protein-protein interactions for p53 function: the CPE contribution. *Protein Eng Des Sel* 24: 41-51.
33. Gill SC, von Hippel PH (1989) Calculation of protein extinction coefficients from amino acid sequence data. *Anal Biochem* 182: 319-326.
34. Delaglio F, Grzesiek S, Vuister GW, Zhu G, Pfeifer J, et al. (1995) NMRPipe: a multidimensional spectral processing system based on UNIX pipes. *J Biomol NMR* 6: 277-293.
35. Schneider CA, Rasband WS, Eliceiri KW (2012) NIH Image to ImageJ: 25 years of image analysis. *Nat Methods* 9: 671-675.
36. Graslund S, Nordlund P, Weigelt J, Hallberg BM, Bray J, et al. (2008) Protein production and purification. *Nat Methods* 5: 135-146.
37. Wong KB, DeDecker BS, Freund SM, Proctor MR, Bycroft M, et al. (1999) Hot-spot mutants of p53 core domain evince characteristic local structural changes. *Proc Natl Acad Sci U S A* 96: 8438-8442.
38. Porath J, Carlsson J, Olsson I, Belfrage G (1975) Metal chelate affinity chromatography, a new approach to protein fractionation. *Nature* 258: 598-599.
39. Pettersen EF, Goddard TD, Huang CC, Couch GS, Greenblatt DM, et al. (2004) UCSF Chimera--a visualization system for exploratory research and analysis. *J Comput Chem* 25: 1605-1612.
40. Sivashanmugam A, Murray V, Cui C, Zhang Y, Wang J, et al. (2009) Practical protocols for production of very high yields of recombinant proteins using *Escherichia coli*. *Protein Sci* 18: 936-948.
41. Bertani G (1951) Studies on lysogenesis. I. The mode of phage liberation by lysogenic *Escherichia coli*. *J Bacteriol* 62: 293-300.
42. Duan J, Nilsson L (2006) Effect of Zn<sup>2+</sup> on DNA recognition and stability of the p53 DNA-binding domain. *Biochemistry* 45: 7483-7492.
43. Lee SH, Ju SK, Lee TY, Huh SH, Han KH (2012) TIP30 directly binds p53 tumor suppressor protein in vitro. *Mol Cells* 34: 495-500.
44. Trinh DL, Elwi AN, Kim SW (2010) Direct interaction between p53 and Tid1 proteins affects p53 mitochondrial localization and apoptosis. *Oncotarget* 1: 396-404.
45. Xu C, Zhao Y, Zhao B (2010) The interaction of azurin and C-terminal domain of p53 is mediated by nucleic acids. *Arch Biochem Biophys* 503: 223-229.
46. Jayaraman L, Moorthy NC, Murthy KG, Manley JL, Bustin M, et al. (1998) High mobility group protein-1 (HMG-1) is a unique activator of p53. *Genes Dev* 12: 462-472.